Influences of black carbon levels in the micro-environment inside urban buses

Anton Dahlberg

Department of Environmental Science

Degree project in Applied Environmental Science 15 credits

Environmental Science

Bachelor Programme in Physics (180 credits)

Spring term 2020

Supervisor: Christer Johansson

Stockholms universitet

Influences of black carbon levels in the micro-environment inside urban buses

Anton Dahlberg

Abstract

Several studies indicate that the cabin of buses is the micro-environment in urban public transport where commuters might be the most exposed to black carbon. Black carbon functions as an indicator of air pollution, which is shown to have harmful impacts on the human body and because it may lead to cancers, systemic inflammation, and cardiovascular diseases, it is listed as one of the top causes to premature deaths, globally. This makes it important to understand what mechanisms there are to the elevated levels of pollutants in urban buses, and by performing mobile in-cabin measurements of black carbon concentrations during 55 bus trips in the public transport system of Stockholm, this study have tried to assess the influences from using different types of fuel, self-contamination, meteorological conditions and driving factors. Although concentrations showed large variability both spatially and temporally, idling at intensely trafficked bus stops showed an average increase of concentrations by 42% compared to the overall average. The risk of allowing increased number of pollutants at bus stops increases with idling for longer time and having the doors open meanwhile.

Keywords

Black carbon, buses, in-cabin, urban air pollution

Contents

Introduction

Background

Air pollution is a serious health issue in today's urban environments. According to the World Health Organization 4.2 million deaths are related to ambient air pollution each year (WHO, 2016). It is also ranked fifth in global burden of diseases (Cohen et al., 2017). Several epidemiological studies have shown that the hazardous properties of air pollution cause damage in the respiratory system and the blood. The issues known to be caused by poor air quality are cardiovascular and respiratory diseases, cancers, and systemic inflammation as well as shortened life-expectancy (Cohen et al., 2017, WHO, 2016, Naturvårdsverket, 2019). The harmful properties are held by small particles called aerosols and especially the ones classified as fine particulate matter with a diameter less than 2.5µm ($PM_{2.5}$). The particles enter the respiratory system, shown in Figure 1, as a constituent of the inhaled polluted air and spreads to various parts of the body.

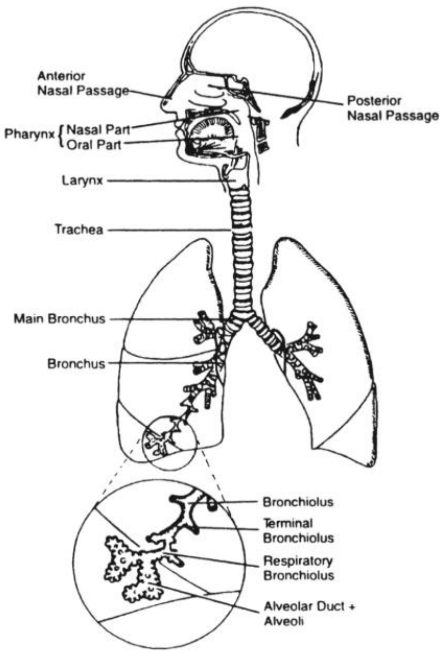

Figure 1. Human respiratory system (Hinds, 1999)

During the breathing process, the airflow experiences many changes in direction on its way through the various parts of the system and particles diffuses onto the walls of the breathing airways at different stages depending on the size and shape of the particles (Hinds, 1999). Large particles (>10µm) carry a lot of inertia and are generally deposited at an early stage of the system like the head airways. The smaller particles (<1µm) can continue without being deposited until they reach the finest part of the respiratory system, the alveolar region of the lung, leading to an increased risk of particles entering the blood system and cause further harm (Hinds, 1999). An atmospheric constituent with established harmful effects on human health is black carbon (Grahame et al., 2014; WHO, 2016). Exposure to black carbon, BC, has been shown to increase the risk in for example lung cancer and ischemic heart disease (Grahame et al., 2014).

Black carbon is a graphitic carbonaceous material in the fine particle range that originates from flames of incomplete combustion processes of carbon-based materials like wood and fossil fuels. BC is a primary aerosol that consists of aggregated small carbon spherules, as can be seen in Figure 2, and are smaller than 0.1µm when they are freshly emitted from a combustion process. The size of the particles is difficult to determine as it varies with time and distance from the source. As the particles cools off, they attract other compounds of organic and inorganic materials which eventually causes them dry deposit due to gravity. The most important sink for BC, however, is wet deposition, and even though BC is a hydrophobic material and is not soluble in water or any of the atmospheric organic solvents (Seinfeld & Pandis, 2016), the compounds it attracts might be and this generates a wet deposition. In general, the estimated atmospheric lifetime of BC lies somewhere between a week and ten days.

Black carbon is named after the particle's most significant property, the ability to absorb light. It is both the most light-absorbing aerosol in the atmosphere as well as the most abundant light-absorbing particle. The particles leave dark stains on filters after deposition, and instruments like the aethalometer can detect the number of deposited particles (Hansen et al., 1984).

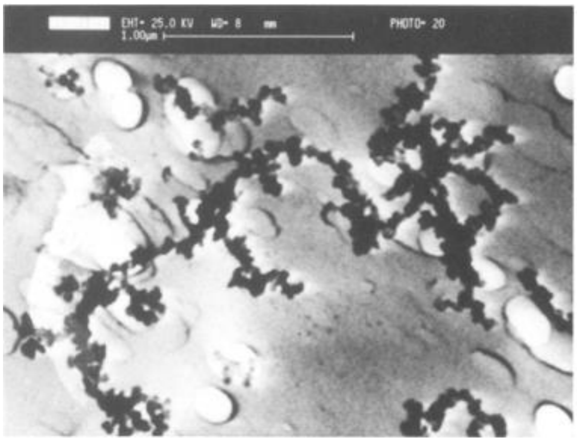

Figure 2. Soot particles on a Nuclepore filter, pictured by Scanning Electron Microscope (SEM) (Fruhstorfer & Niessner, 1994).

The health issues linked to BC and air pollution is a problem in urban environments, where emissions primarily come from traffic, and have been addressed as a threat to public health by WHO (2016). Since BC is emitted from known anthropogenic sources and possess the light-absorbing properties to make it easy to quantify, it functions as a good indicator of air quality and is therefore widely measured in air pollution studies (Bond et al., 2013).

Studies made in different cities around the world have found that commuters in the public transport are the most affected of poor air quality (Targino et al. 2018, Carvalho et al. 2018, Ham et al. 2017, Zuurbier et al. 2010, Morales et al. 2019, Nogueira et al. 2019, Merritt et al. 2019). The studies have attempted to assess the exposure of BC and $PM_{2.5}$ for people living in urban environments while using different ways of transportation within the cities and the studies compare exposure during different modes of transport like bus, car, walking and cycling. Consistently the measurements of exposure for those who travel by bus are the highest except in one case that included train as a mode of transport (Ham et al., 2017). The studies suggest different reasons to the high in-cabin exposures in buses but none of the studies have tried to fully explain this since the aim has been to investigate personal exposure.

At bus stops, the surrounding polluted air can enter the cabin as doors open to let passengers in and out, this is established as a contributing factor by Ham et al. (2017). On the contrary, other research has shown higher concentrations inside buses than outside (Betancourt et al., 2019; Zuurbier et al., 2010). This leads to driving factors like driving in traffic situations with many red lights and intersections compared to higher speeds without stops has been established as a reason to increased concentrations (Targino et al. 2018; Zuurbier et al. 2010).

The choice of fuel to run the bus has shown to have impact on the in-cabin exposure of air pollutants. Some studies have researched the differences between bus models and found that diesel driven buses of old euro classes give extensively higher exposures of BC than more modern euro classes and electrically driven buses (Zuurbier et al. 2010; Morales Betancourt et al. 2019; Nogueira et al. 2019). The study by Zuurbier et al. (2010) found that concentrations of BC were 46% higher inside a diesel driven bus compared to inside an electric. Targino et al, (2020) assessed the difference between buses driven with diesel compared to biodiesel and found significant reductions in exposure inside biodiesel as compared to diesel.

The choice of fuel would also support the idea of self-pollution. Self-pollution is the mechanism that pollutants from the bus's own exhaust enter the cabin, and is suggested as an explanation to the differences in in-cabin concentrations between fuels (Zuurbier et al. 2010; Morales Betancourt et al. 2019;Nogueira et al. 2019; Targino et al, 2020). As more pollutants will be emitted by a bus fuelled with for example fossil fuel than an electric bus, more pollutants are going to enter the cabin if self-pollution is occurring. The air from the own exhaust may enter through the windows and doors at bus stops or also through gaps in the floor (Behrentz et al. 2004). A few studies have tried to investigate the occurrence of self-pollution in relation to driving speed and idling with different set ups (Behrentz et al., 2004; Li et al., 2017; Zhang et al., 2013). Driving speed have shown to have significant impact on the turnover time for the air inside the buses with impacts on concentrations following with it (Li et al., 2017). While idling, it is suggested that during specific meteorological events, self-pollution takes place, these studies are not tested in real-traffic environments but rather in carefully set up tests (Behrentz et al., 2004; Zhang et al., 2013).

Driving with open or closed windows has been shown to impact the concentrations with high variability. Li et al., (2015) relates high in-cabin concentrations with open windows but studies opposing this view (Behrentz et al., 2004; Li et al., 2017) also exists, making this an understudied subject with regard to buses leaving room for improvement in the understanding.

Motivation and aim of this study

The primary aim of the studies that have tried to assess exposure during different modes of commuting has been to establish the timing and choice of mode that exposes commuters to an increased risk of inhaling polluted air. Together with the research on self-pollution that is not performed in real traffic situations, this shows that it is not well-studied what the causes are of the elevated concentrations of air pollutants inside buses during real traffic situations. In an attempt to get a better understanding of why buses are the most polluted choice of commute, the objective of this study is to i) compare the in-cabin concentrations between buses with high, biodiesel, and low, biogas, emissions of BC ii) explore what factors there are that control the micro-environment inside buses and to what extent the influence from these factors are.

Material and Methods

Study design

In Figure 3 the selected bus route for the study is shown, a densely trafficked route running from Stadion to Skanstull, with number of vehicles on the route ranging from 8,000-28,000 (Stockholm Stad 2020). This route was selected because of the length in time it takes to travel between the stations, the close interval in departures of buses and the mix between the two fuels. It takes approximately 40 minutes to travel the 9.6 km route which is similar to the average time a public transport commuter in the Stockholm region spend on one trip (SL, 2018). Buses in this route run in an interval of 4-6 minutes throughout the day which makes the sampling sessions more effective by avoiding long waiting time between bus rides. The close interval of departures also contributed to getting samples of similar ambient BC concentrations and variations along the route. However, the most important factor to select this route is the mix between buses running with both biogas and biodiesel, around every second bus is run with different fuels. The two fuels are selected because the emissions of BC from biogas and biodiesel differs, which enables the opportunity to compare different fuels. Further details on the fuels are presented in the following sections. There is no exact official statistic for the distribution of buses since the traffic operators use an advanced data algorithm to allocate buses to the different routes causing a day-to-day variation in bus type (SLL 2020, personal communication, 17 March).

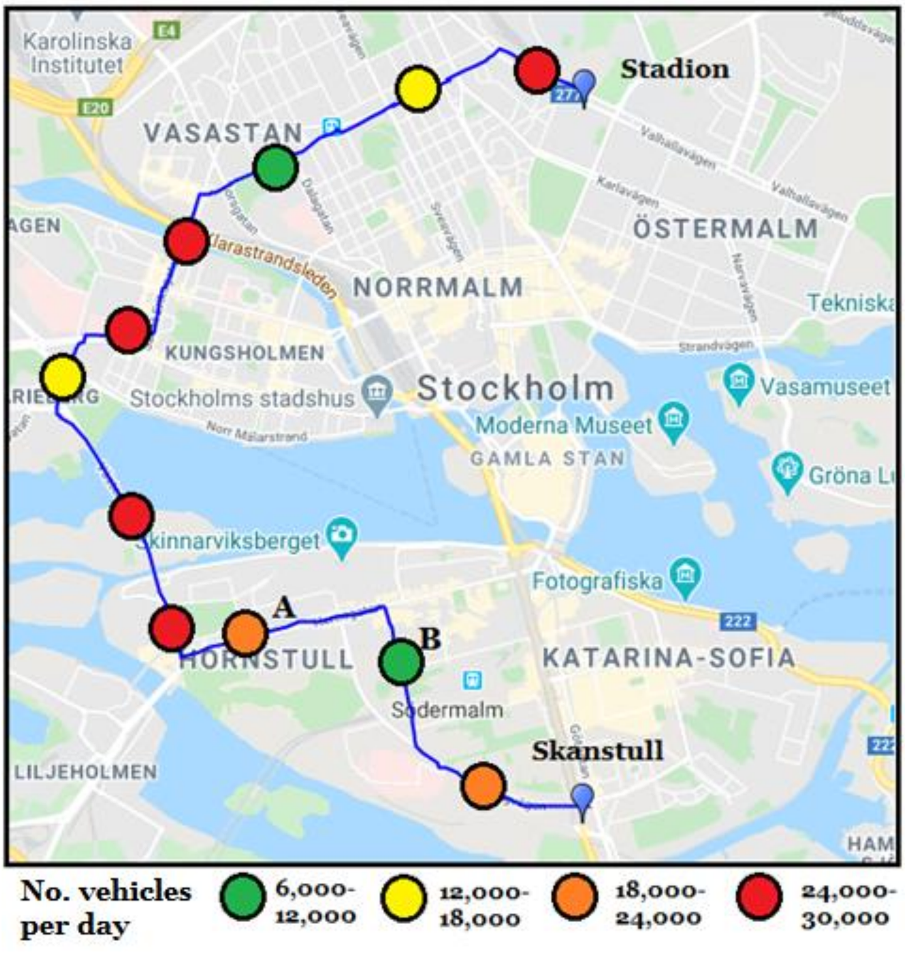

Figure 3. An overview for the trip of the measurements. Coloured dots represent traffic intensity averages. At location A, ambient street level concentrations are measured. At location B, urban background concentrations are measured at Torkel Knutssongatan.

Experimental approach

Measurements of BC concentrations were conducted using two portable aethalometers of a model called Microaeth AE51 from Aethlabs in California, USA. The AE51 is in the dimensions 117mm × 66mm × 38mm and a weight of 0.280kg, a size suitable for making mobile measurements without carrying too much load. Airflow Q and resolution time Δt can be adjusted by the user and in this study an airflow of 100 ml/min and a time resolution of 10s was used to get good sensitivity in the measuring campaigns as well as effective use of battery life. This is in accordance with recommendations from the manufacturer for air pollution measurements in traffic. To assure the quality of the measurements and avoid the risk of not being able to sample data if the instrument fails, two aethalometers were used in every sampling session. They were brought along in a backpack with the air-flow inlets pointing out from the top of the backpack. During trips, the position inside the bus was held to the same seat to the most possible extent, it sometimes differed a little bit depending on the design of the bus and amount of people inside. This position was approximately 2.5 meters from the closest door pair and in the back of the bus. The backpack was held in the lap with the inlets of the tubes pointing forward and within the 30cm breathing zone hemisphere to get a realistic approximation of exposure and dose during the trips.

A logbook was carried to note any events of potential impact on the results like: windows opened or closed, bus driver change causing a long hold at a station or if many stations were passed by, not allowing new air enter the bus.

During each trip, a GPS logger (Renkforce GT-730FL-S, Germany) was used to register the path and length of each trip to later be matched with the sampled data to get an image of how the concentrations vary spatially.

Studied buses

The study was performed in Stockholm, Sweden where the public transport fleet of buses consists of 2202 buses where 75% run on biodiesel, Hydrogenated vegetable oil, HVO, and Rapeseed Methyl Esters, RME, 15% biogas and 10% ethanol (SL, 2018). The two fuels compared in this study are biogas and biodiesel. The biogas buses either run on methane from Compressed Natural Gas (CNG) which is a fossil fuel, or biogas that is produced from different biogas plants in the Stockholm region. The emission standard of biogas buses is classified as enhanced environmentally friendly vehicles, EEV. All the biodiesel buses operating in this study are of class Euro VI which put the highest demands in particulate filters of the present classes. By identifying the license plate of the bus at each trip, information from the bus manufacturer could be attained. Emission factors for black carbon of the buses included in the study are showed in Table 1 and has been retrieved from the HBEFA 4.1 database. The estimations of emission factors and fuel consumptions are based on a saturated traffic mode implying an average driving speed of 22.4km/h, very similar to what was measured in this study.

Emission Factors (EF) for sampled buses				
Fuel	Number	Year	EF_{BC} $\left[\frac{mg}{km}\right]$	$Q_{exhaust}^{a}\left[\frac{l}{min}\right]$
Biodiesel (Euro-VI)	15	2014	4.46	9338
Biodiesel (Euro-VI)	3	2015	4.46	9338
CNG (EEV)	7	2011	1.06	9113
CNG (EEV)	7	2014	1.06	9113
CNG (EEV)	5	2018	1.06	9113

Table 1. Summary of buses used in the study. [a] Volumetric flow rate for diesel buses with retrofitted particulate filter and for CNG buses of older year (Behrentz et al., 2004)

Calculations of in-cabin concentrations explained by emissions from the vehicles own exhaust uses the emission factors provided by HBEFA 4.1 and the volumetric flow rate from the exhaust calculated by Behrentz et al. (2004). Mass flow rate of BC is calculated with the known average length of the trips, $\overline{d}$, and the average time elapsed on a trip, $\overline{\Delta t}$. By dividing the mass flow rate of black carbon, $\mathrm{M_{BC}}$, with the volumetric flow rate of air from the exhaust, $Q_{exhaust}$, the concentrations of BC in the air from the exhaust is found.

$$\mathrm{M_{BC}} = \frac{\mathrm{EF_{BC}}\left[\frac{\mathrm{mg}}{\mathrm{km}}\right] \times \overline{d}[km]}{\overline{\Delta t}[min]} \qquad (1).$$

$$C_{exhaust} = \frac{M_{BC}\left[\frac{mg}{min}\right]}{Q_{exhaust}\left[\frac{l}{min}\right]} \qquad (2).$$

The aethalometer

The aethalometer was first described by Hansen et al. (1984) and operates by pumping the particle containing air through an electrically conductive tube to avoid losses to diffusion, the air then flows through a filter of T60 (Teflon-coated borosilicate glass fibre) material where the aerosol is deposited on a circular area A with a radius of 3mm. Since different kinds of particles in the aerosol will enter the tube, the aethalometer need a method to distinguish the BC particles from others and does so by exploiting the optical properties of BC. The black coloured particles blacken the colour of the originally white filter in A, and this process is strengthened continuously along with the time of the measurement. As the area grows darker, an unaltered monochromatic light source at wavelength λ=880 nm that illuminates the area will experience a continuous reduction in transmittance as time pass. The wavelength has been empirically determined to be the most absorbed by BC and makes sure that other particles does not reflect the light. The aethalometer measure the reduction in transmission by comparing a reference value without any loading of BC with intensity I_0 and the intensity at a time later I. This process of reduction in transmission is called attenuation of light ATN and is described by the alternative form of Beer-Lambert law which relates the change in attenuation to a material's properties:

$$\mathrm{I} = I_0 e^{-\left(\frac{\mu_a}{\rho_m}\right)\sigma} \qquad (3).$$

Where μ_a [m^{-1}] is the absorption coefficient, and ρ_m [kgm^{-3}] is the mass density of the material. $\frac{\mu_a}{\rho_m}$ [m^2kg^{-1}] then becomes the mass absorption coefficient.

σ [kgm^{-2}] is the area density of the material and relates the mass density and the length that attenuation takes place, l, of the material $\sigma = \rho_m \mathrm{l}$. By doing the natural logarithm of Beer Lamberts law an expression for attenuation is attained:

$$ln\left[\frac{I}{I_0}\right] = \left(\frac{\mu_a}{\rho_m}\right)\sigma = ATN \quad (4).$$

This can used to calculate the concentration of BC, C, by relating the change in attenuation, ΔATN, over the specified timestep.

$$\frac{\mu_a}{\rho_m}\frac{\sigma}{\Delta t} = \frac{\Delta ATN}{\Delta t} \qquad (5).$$

Since σ can be written as $\frac{m}{A}$ and ρ_m as $\frac{m}{V}$ the expression can be rewritten as:

$$\mu_a = \frac{\mathrm{A\Delta t}}{\mathrm{V}} \times \frac{\Delta A\mathrm{TN}}{\Delta \mathrm{t}} \quad (6).$$

inserting $\mathrm{Q} = \frac{V}{t}$ gives an expression for the attenuation coefficient:

$$\mu_a = \frac{\mathrm{A}}{\mathrm{Q}} \times \frac{\Delta A\mathrm{TN}}{\Delta \mathrm{t}} \quad (7).$$

The relation $C_{BC}\epsilon = \mu_a$, where ϵ [m^2g^{-1}] is the attenuation cross section or mass absorption efficiency provides the expression for concentration:

$$\mathrm{C_{BC}} = \frac{\mathrm{A}}{\mathrm{Q}\,\epsilon} \times \frac{\Delta A\mathrm{TN}}{\Delta \mathrm{t}} \quad (8).$$

The ϵ is a wavelength dependent constant and is determined by the manufacturer to be 16 m^2g^{-1} for aethalometers operating with wavelength 880nm.

The aethalometers used in this study:

A bivariate orthogonal regression analysis was used to determine how well the aethalometers correlated and is visualised in Figure 4. The data from the test is summarised in Table 2 and a plot for how well the instruments correlated during the campaign is visualised in Figure 5. Even though the meters do not show exact equal values, they correlate well in rises and falls in concentration which is the most important in this study since it is a study of what influences the increases and decreases of concentrations inside buses.

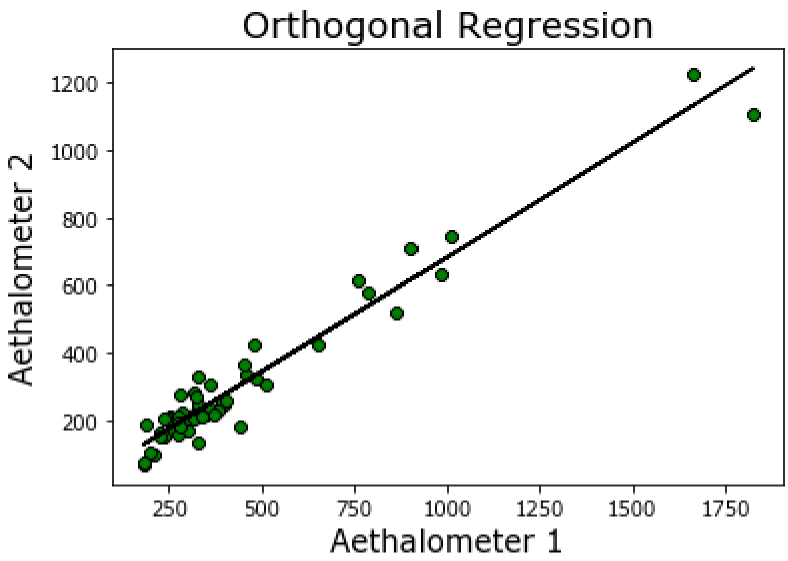

Figure 4. Orthogonal regression between the two aethalometers.

Aethalometer test					
Statistics		Aethalometer 1		Aethalometer 2	
Mean		439		303	
SD		325		225	
Correlation	0.97	y-intercept	-0.055	slope	0.69

Table 2. Statistical parameters from the aethalometers used in the study.

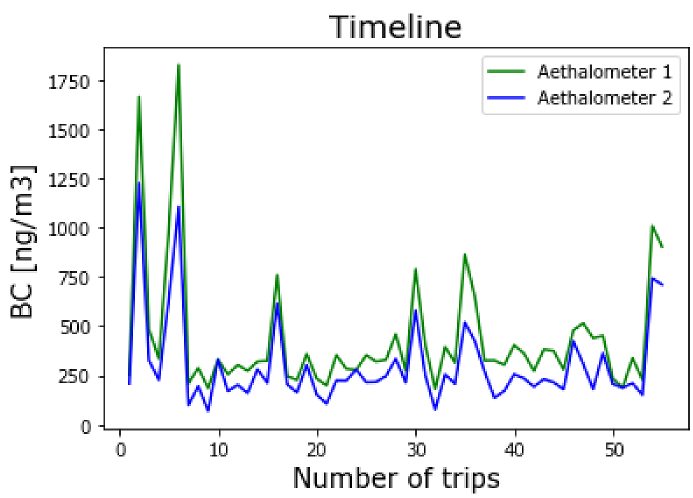

Figure 5. Timeline for the means of the measurements visualising the correlation through the campaign.

Post-processing of sampled data

Each datafile from the aethalometers were post-processed by a software program provided on the website from Aethlabs. The selected method of noise reduction is the Optimized Noise-Reduction Averaging (ONA), a method developed by Hagler et al. (2011). ONA is an algorithm that extracts data for attenuation, BC concentrations and time interval settings to adjust inadequate changes in attenuation, an issue that is very common with aethalometers. Especially in environments with low levels of BC concentrations because the change in attenuation can at times be too small to detect for the meter, this leads to an increased influence of noise levels and gives rise to negative values in BC concentrations (Hagler et al., 2011). Because of the negative values, high positive peaks appear when the attenuation finds its way back to the regular trend. The purpose of ONA is to eliminate the negative values and at the same time avoid the peaks which in turn generate a less fluctuant data set and assures the quality of the data. ONA works by first allowing the user to manually specify a minimum change in attenuation $\Delta \text{AT}N_{min}$ for each time step, in this study a minimum change of 0.01 was used in accordance with the recommended settings from Aethlabs. The algorithm run through the data file and at a row where the attenuation does not match the specified requirement, $\Delta A\text{TN} \geq \Delta A\text{TN}_{min}$, it continues to the next row that meets it. At this point, the algorithm averages the BC concentrations for the number of rows it skipped and assigns the mean to all rows. This is repeated throughout the file, and in this way, ONA smoothens the data set and provides a more reliable set of concentrations.

Data analysis

The structure of the data analysis was divided into 4 steps.

(1) After each measuring session the arithmetic mean, median and percentiles was calculated for each trip separately.

(2) For all trips with the same fuel the concentrations were averaged using a weighted average eq (9) to consider the differences in time spent on each trip, the same method was used for dose and exposure.

(3) When the data sampling campaign finished, 4 data sets were produced consisting of averages for every 10s timestep from all sampling sessions. The data sets were biogas trips from Stadion to Skanstull, biogas trips from Skanstull to Stadion, biodiesel from Stadion to Skanstull and biodiesel from Skanstull to Stadion. The data was matched with the GPS data in gpsvisualizer.com.

(4) Calculations of the totals from all sessions.

$$\text{Weighted average} = \frac{\sum_{i=1}^{n} w_i \, x_i}{\sum_{i=1}^{n} w_i} \quad , \text{w = length of trip, x = mean concentration} \qquad (9)$$

All data from the aethalometers were imported as csv files and then handled in programming language Python, Microsoft Office Excel and JMP for making plots and statistical evaluations. The printed maps matched with concentrations are visualised with the help of gpsvisualizer.com after processing the GPS data and sample data with Python code (gpsvisualizer.com).

The Mann Whitney U test is a non-parametric test for examining whether two independent non-normal distributions are equal or not. The null hypothesis is that the distributions are equal. The test provides a U-statistic that tells how many times a number from one of the distributions is smaller than a number in the other distribution. A low U-statistic generally indicates that the samples significantly differ. To determine whether the test is significant, a p-value compares the U-statistic with the Z-distribution for the number of elements in the list, if the achieved U is larger or smaller than the Z for the tested significance level, the p-value will be small and thus reject the null-hypothesis.

The Kruskal Wallis test is an extension of the Mann Whitney U test that allows three or more distributions to be compared in the same test with the null hypothesis still being that the samples origin from the same distribution. It generates an H-statistic instead of a U, which comes from a chi-squared distribution instead of a Z-distribution.

Spearman rank correlation test is a monotonic and non-parametric measure of how well two data sets are associated with each other. By quantifying the association from a number between +1 to -1 where +1 is perfect positive association and -1 perfect negative association.

Ancillary data

Ambient and background concentrations

Access to data of ambient BC concentrations was provided by Stockholm Luft och Buller (SLB) and Miljöförvaltningen (SLB analys). The concentrations were downloaded in files from their webpage and processed to both correlate with aethalometer data as well as show differences in concentrations. The measurements are hourly averages and measured with a wavelength of λ=880 nm. Concentrations of ambient street level are measured at Hornsgatan and urban background on the roof top of a building at Torkel Knutssongatan, both places are highlighted in the map in Figure 1.

Meteorological data

Temperature, relative humidity, precipitation, wind speed and wind direction were accessed at the urban background measurement station at Torkel Knutssongatan and consisted of hourly averages.

Surrounding traffic

Traffic rates for all streets was provided by Stockholm Stad (2020) with daily average numbers of vehicles and how large part are heavy duty vehicles from measurements made in 2014.

Results

The study collected samples of BC concentrations on 14 sessions, providing data from 55 bus trips with 28 and 27 trips fuelled with biodiesel and biogas, respectively. All sampling sessions were kept to the same time span, 9.45-13.00, and consisted of one trip in each direction with both fuels. The average time spent in a trip was 36 min where the shortest was 30 min and the longest 43 min.

Spatial Variability

The synchronisation of time steps between GPS points and aethalometer data resulted in a time-dependent spatial distribution, visualised in Figure 6. In the plots of the spatial distributions, four places of interest (A-D) have been marked and are referred to as “Hot spots” in Table 3 in which a statistical summary of concentrations is presented.

Since time spent on each trip varied, the figures are not representative in context of exact concentrations, but they serve as an estimate of where an increase in concentrations occurred along the travelled path. To test correlations between the trips, a Spearman correlation test with significance level $\alpha=0.05$ was performed and resulted in; biogas in each direction $\rho=0.58$ with p-value 0.04 and biodiesel in each direction 0.19 with p-value 0.52. This means that the biogas cannot be rejected as uncorrelated, although the test is not very strong. The biodiesel trips show very little correlation and is not suggested to correlate according to the test-statistic.

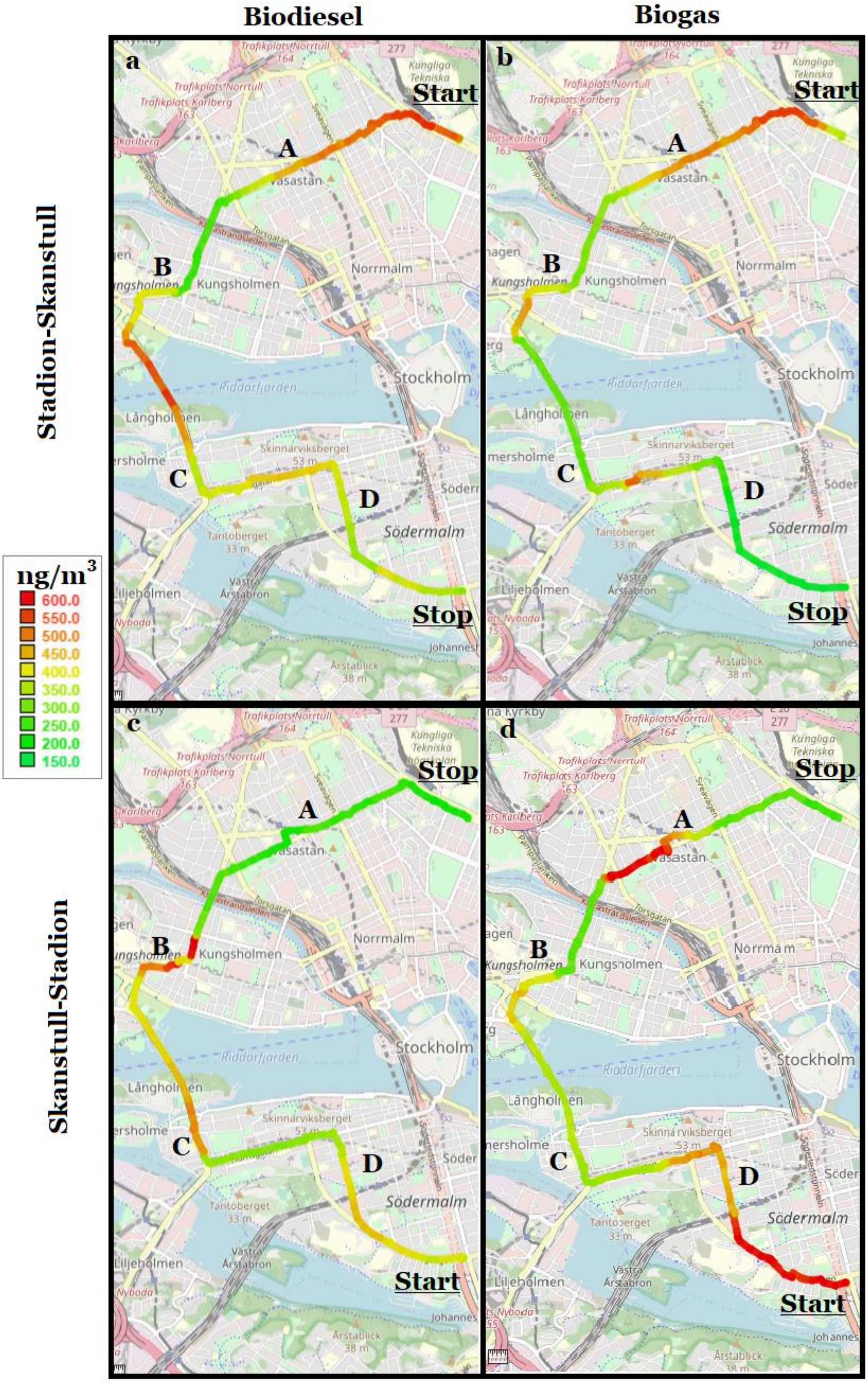

Figure 6. Illustration of spatial variability of BC concentrations along bus routes. A. Odenplan. B. Fridhemsplan. C. Hornstull. D. Södra Station. a: biodiesel in direction towards Skanstull, b: biogas towards Skanstull, c: biodiesel towards Stadion, d: biogas towards Stadion.

The selection of bus stops as "hot spots" was made by observing repeated prolonged stops of about 1 minute or longer at the same station, the data presented in Table 3 is a statistical summary of concentrations in these places compared to concentrations from the entire campaign. Compared to the overall totals, the mean concentrations at the locations are all higher in absolute numbers and the percentage difference is 102%, 22%, 35% and 12% higher for Odenplan, Fridhemsplan, Hornstull and Södra Station, respectively. Number of vehicles driving by a hot spot daily is presented in the last row of Table 3 where the 8,000 vehicles at Södra Station (E) differ significantly from the others but still experience similar average concentrations.

	Hot spots				
Statistics	Odenplan (**A**) n = 6	Fridhemsplan (**B**) n=16	Hornstull (**C**) n=6	Södra Station (**D**) n=6	Overall Total
P5	304	112	281	189	72
P25	338	260	337	367	156
Median	487	331	412	407	250
P75	866	494	499	539	420
P95	1652	1117	912	581	1,053
Mean	739	447	496	411	366
SD	557	409	257	151	390
Maximum	1878	1874	1043	581	8,740
No. vehicles per day (heavy duty vehicles)	15,250 (10%)	26,000 (8%)	28,000 (10%)	8,000 (12%)	-

Table 3. Statistical summary of concentrations in ng/m³ for hot spots. In the top row: Name of bus stop, (Location in Figure 6), n=number of stops.

The relation between speed and concentrations from a randomly selected trip is plotted in Figure 7. Increased values are seen at the start, where many starts and stops take place, and during a long stop in minute 25. The elevated values for start and stop driving is not repeated by the end of the route.

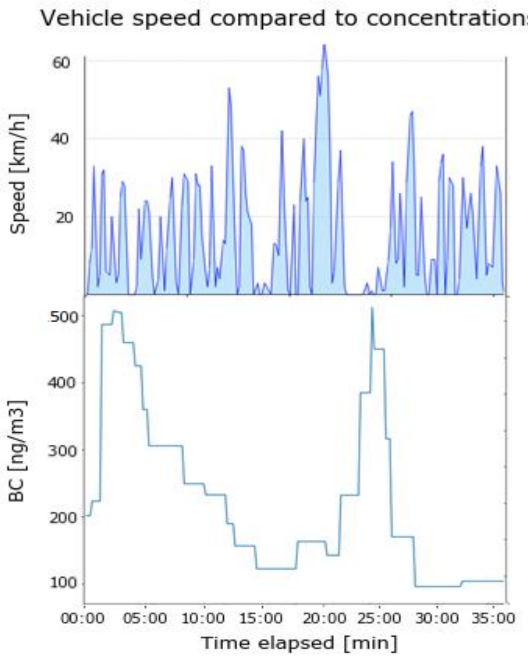

Figure 7. Relation between speed and concentrations.

Daily variability

The daily variation between the trips in each direction with each fuel visualised in Figure 8 show that there are no regular patterns of the variability between trips except that the measurements in general are consistently close to the ambient street level concentrations. Figures 8b 8e 8f 8g 8m, display cases where only one trip distinguishing itself from the other trips on the same day, indicating that certain events occurred during the trip that could explain the variation.

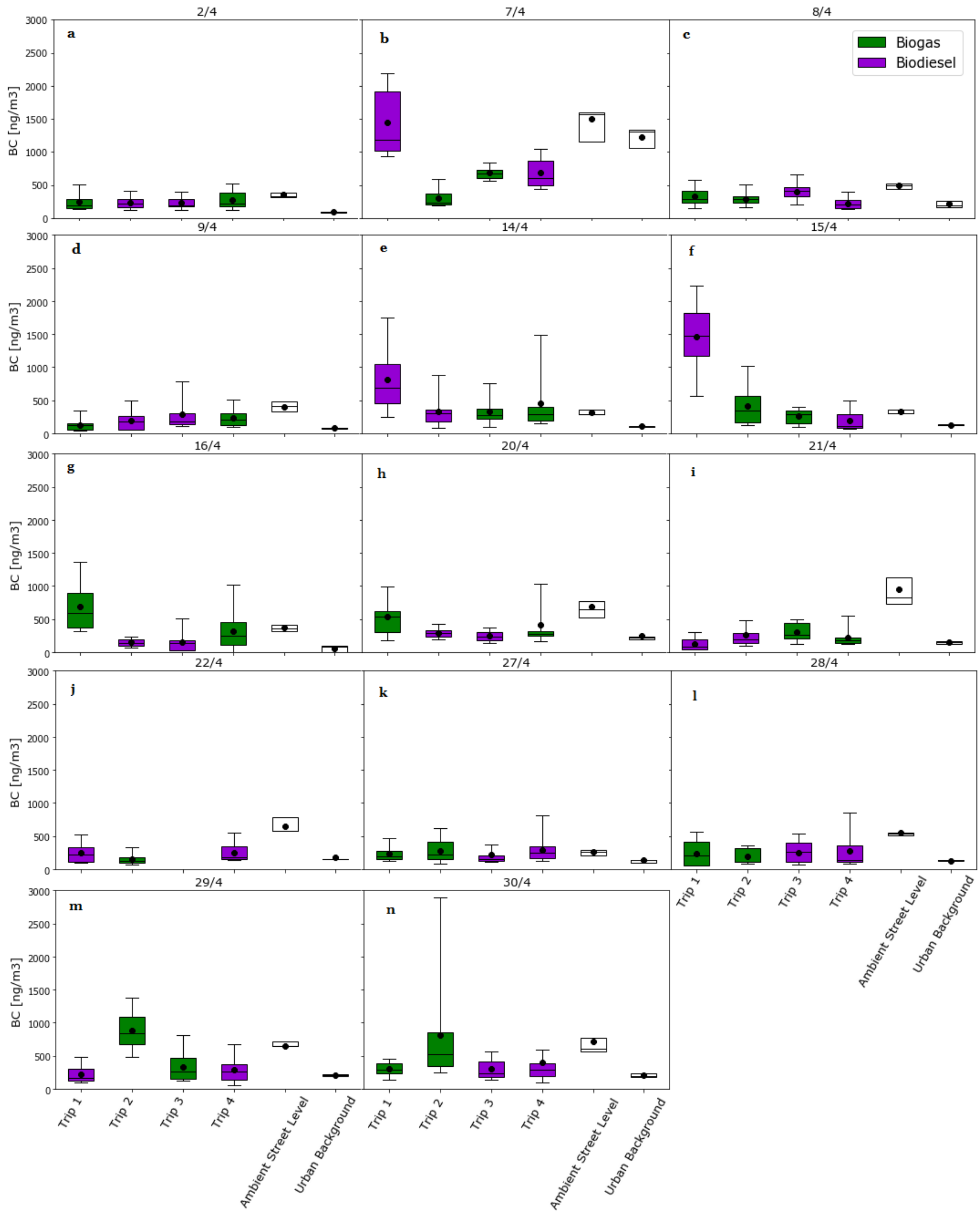

Figure 8. Box plots for the daily variation. Orange line represents median, green dot represents mean, the boxes marks the interquartile boundaries (25th and 75th percentile) and the whiskers the 5th and 95th

percentile. The plots (a-n) are sorted chronologically trip on the x-axis. A statistical summary of the plots is found Table 7 in Appendix A.

A Kruskal Wallis test between the 14 days with: 13 degrees of freedom (k-1), significance level of α=0.05 and a critical chi-squared value of χ^2=22.819, resulted in H = 2363 and p-value < 0.05. Since the obtained value of H is larger than χ^2, the null hypothesis is rejected and suggests that there is a significant statistical difference between the distributions of the days.

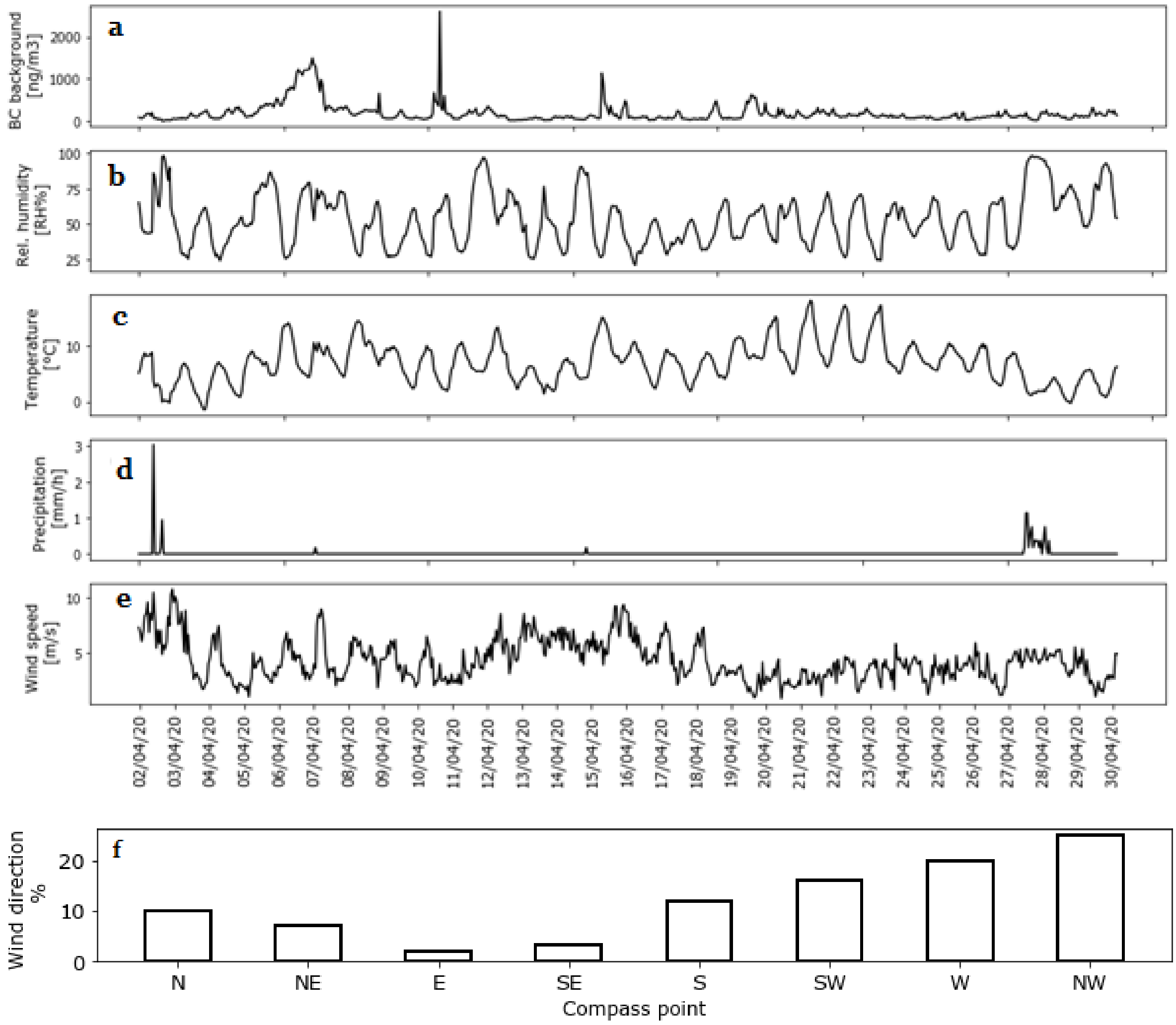

Figure 9. Daily variation of meteorological parameters and urban background measurements for the period of the campaign. a: BC background, b: relative humidity, c: temperature, d: precipitation, e: wind speed, f: wind direction. All data is received from SLB (2020).

In general, the period of the sampling campaign consisted of sunny, dry, and windy days where relative humidity (Figure 9b) and temperature (Figure 9c) showed a variation ranging between 30% - 60%, except for days with rain, and 2°C and 14°C respectively at noon. Temperature however, showed a decline in the last days of the campaign to an interval of 2°C to 6°C along with increasing relative humidity. Wind speeds (Figure 9e) experienced daily variation through the period, ranging from 1 – 8.5 m/s for measurements at noon. Rainfall (Figure 9d) only occurred on two occasions during active sampling sessions and during nights on three occasions. The measurements of background concentrations (Figure 9a) shows an irregular pattern of peaks but can be correlated with data for wind directions. Where peaks in concentration occurs, wind direction ranges between SE (160°) and SW (200°). Even though wind direction changes rapidly through the day, a general frequency distribution of wind directions during the period is shown in the bar plot in Figure 9f. The most frequent directions are those of westerly origin constituting around 60% of the data points.

Diurnal variation

The average meteorological variations during the day were consistent, experiencing decreasing relative humidity (Figure 10a), increasing temperature (Figure 10b) and increasing wind speed (Figure 10c). Relative humidity starts in a high value and decrease constantly through the day, except on days with rainfall. Together with increasing temperatures, wind speed (Figure 10c) increases as the warming of air establish heat-gradients which causes the air to move more turbulently. The BC concentrations (Figure 10d) measured at the urban background site experienced a daily decline in numbers through the days.

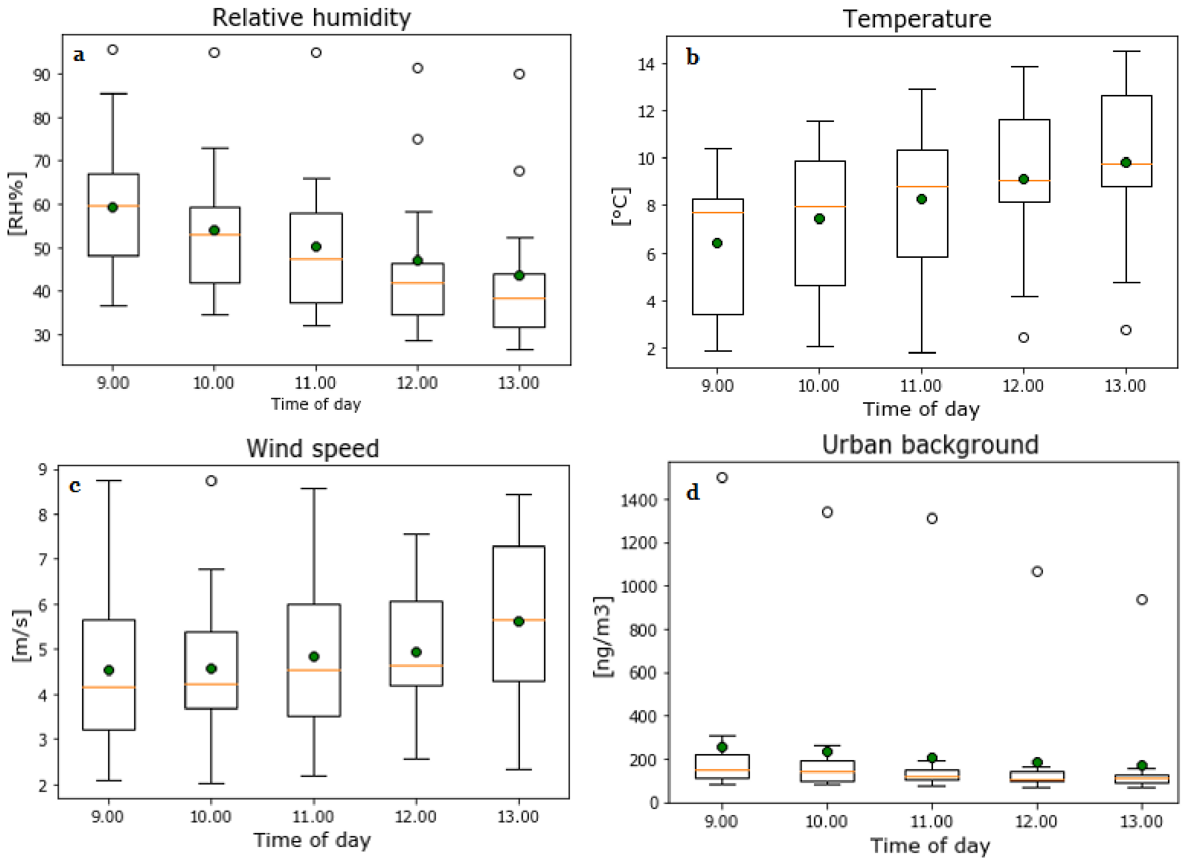

Figure 10. The average diurnal meteorological variations for days when sampling was performed and the urban background measurements. Orange line represents median, green dot represents mean, the boxes marks the interquartile boundaries (25th and 75th percentile) and the whiskers the 5th and 95th percentile. Dots represent outliers.

The distributions of number of trips during the campaign's four different time intervals shown in Figure 11ab shows that biogas-trips where more common in the first two sessions and biodiesel in the last two. Largest difference is found in biogas with five trips in the time-interval 11.20 to 12.10 compared to 8 trips in both 9.40-10.30 and 10.11.20.

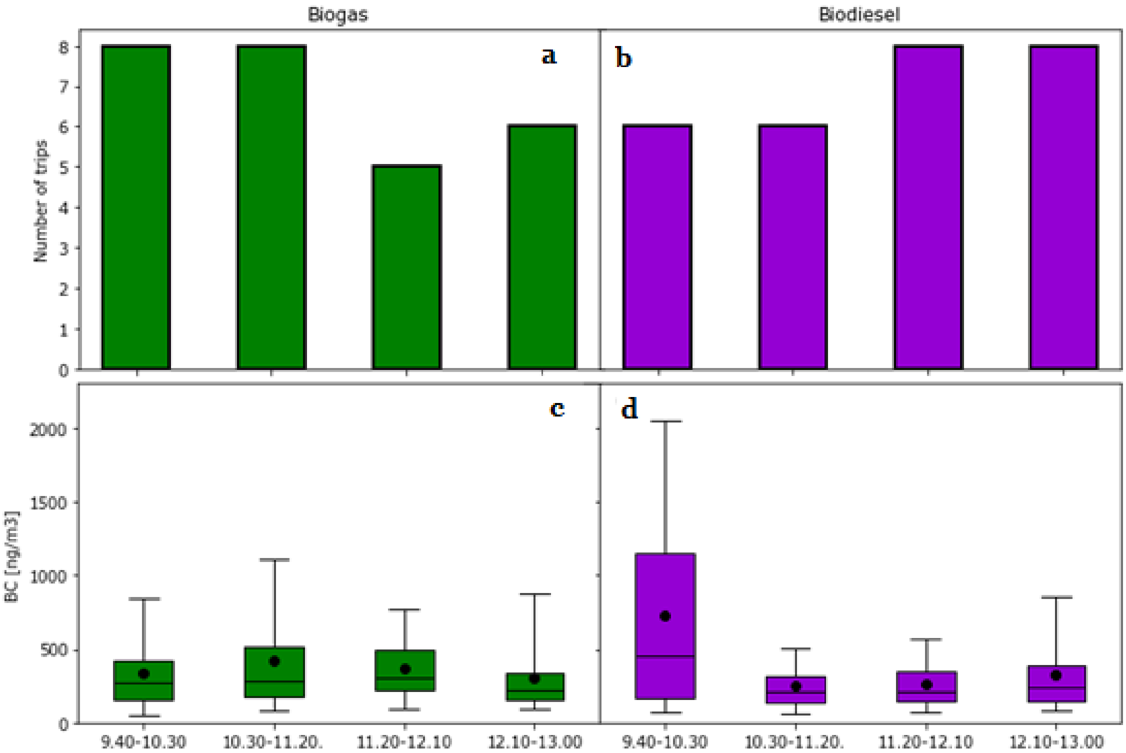

Figure 11. Left side (a & c): Bus trips with biogas. Right side (b & d).: Bus trips with biodiesel. Top panel (a & b): Distribution of number of trips performed in the specified daily time intervals. Bottom panel (b & d): Box plots displaying the variation in the time intervals. Box plots: Black line represents median, black dot represents mean, the boxes mark the interquartile (25th and 75th percentile) boundaries and the whiskers the 5th and 95th percentile.

The concentrations in the boxplots of Figure 11cd are based on the mean values for all trips in every time-interval and show little variation for trips running with biogas (Figure 11c). In Figure 11d, trips with biodiesel that were sampled in the first time-interval significantly differs from the other. The large increase in morning trips is strongly influenced by three trips performed on the seventh, 14th and 15th as can be seen in in Table 4 where further details on all morning trips with biodiesel are presented.

Biodiesel - early trips						
Parameter	7/4	14/4	15/4	21/4	22/4	29/4
$Mean_{trip}$ [ng/m^3]	1145	806	1466	128	245	217
$Mean_{day}$ [ng/m^3]	780	479	583	224	308*	428
Street level [ng/m^3]	1600	240	310	830	580	710
Background [ng/m^3]	1440	90	140	160	155	190
WD [°]	200-230	305-315	280-305	330-350	2-14	330-340
WS [m/s]	3-4	6-7	6-7	2-4	2-4	4
No. Long stops	0	1	2	1	2	2
Sun roof	Closed	Closed	Open	Closed	Closed	Closed

*Table 4. Summary of parameters affecting the morning trips for biodiesel. *includes three trips instead of four.*

Differences between studied buses

The box plot in Figure 12 shows a comparison between biogas and biodiesel with trips in both directions included in each fuel. The only significant difference between the fuels is the skewed distribution of biodiesel that indicate that it includes a larger number of high values than biogas.

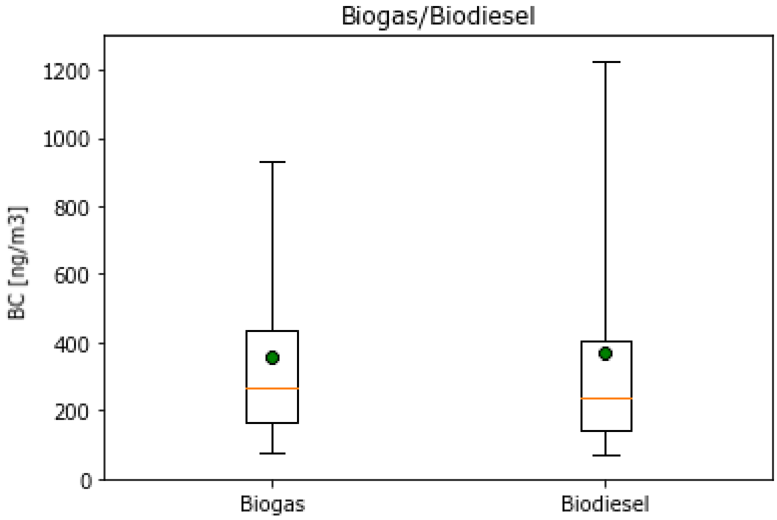

Figure 12. Box plot for trips with biogas and biodiesel. Orange line represents median, green dot represents mean, the boxes marks the interquartile boundaries (25th and 75th percentile) and the whiskers the 5th and 95th percentile.

Data from the box plot in Figure 12 is presented in Table 5, quantifying the skewed distribution showed in the figure. The mean concentration for trips made in buses fuelled with biodiesel is 3.6% higher than those made in a biogas bus. The peak concentration of biodiesel, however, exceeds biogas with 91%.

	Difference between fuels	
Statistics	Biogas [ng/m^3] (n=27)	Biodiesel [ng/m^3] (n=28)
P5	74	70
P25	169	143
Median	266	237
P75	433	407
P95	929	1,223
Mean	359	372
SD	345	427
Maximum	4,580	8,740

Table 5. Statistical summary for means from all trips with each fuel.

To consider that the length of the trips varied and the difference in number of trips, 28 and 27, a weighted average for the two fuels was calculated as well and resulted in no significant difference, weighted average for biogas trips resulted in 358 ng/m^3 and biodiesel 374 ng/m^3.

The concentrations of BC in the exhaust air is calculated using eq. (1) and (2) and resulted in 31,000 ng/m^3 for biogas and 127,000 ng/m^3 for biodiesel. All the exhausted BC will not enter the cabin and Behrentz et al. (2004) found that approximately 0.03% of exhausts from the plume enter the cabin during a trip, the fraction that enters the cabin is denoted θ. Calculations of concentrations entering the cabin using $\theta = 0.0003$ resulted in 9 ng/m^3 for biogas and 38 ng/m^3 for biodiesel, this corresponds to 2.5% and 10% of the mean concentrations.

The Mann Whitney U test between the fuel types resulted in; U =16,875,798 and p-value=$8.16e^{-13}$. The critical U for this sample is 17,963,555 which is larger than the obtained U and rejects the null hypothesis, suggesting that the distributions of the samples are unequal.

Despite the generally cold weather during the measurement campaign there were some occasions on which where the windows of the bus were open. The distribution of trips with closed windows and trips with open windows are visualised in Figure 13. There is a skewed distribution and higher mean in concentrations when the sunroof is open compared to closed.

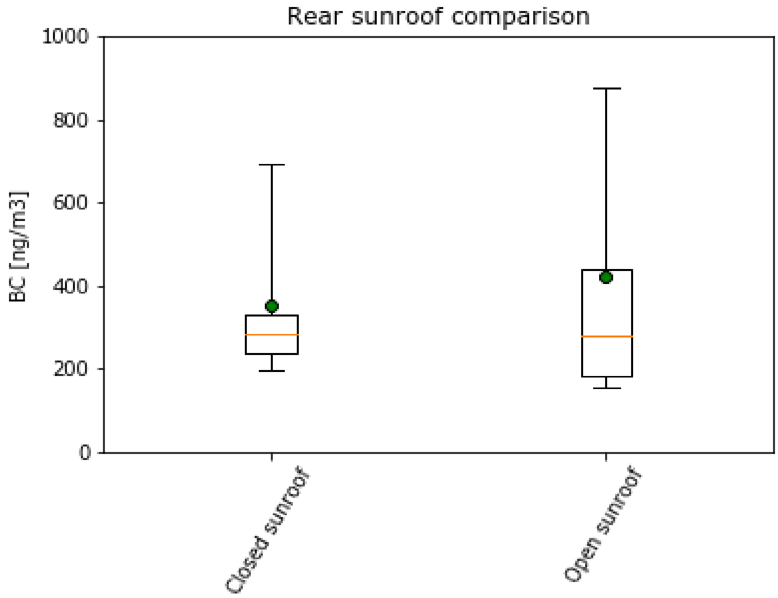

Figure 13. Comparison between trips with open or closed sunroof. Orange line represents median, green dot represents mean, the boxes marks the interquartile boundaries (25th and 75th percentile) and the whiskers the 5th and 95th percentile.

Open/closed sunroof		
Statistics	Closed [ng/m^3] (n=43)	Open [ng/m^3] (n=12)
P5	190	154
P25	235	185
Median	282	277
P75	328	439
P95	795	1142
Mean	353	421
SD	234	373
Maximum	1445	1466

Table 6. Statistical summary of trips with closed and open sunroof. n= number of trips.

The Mann Whitney U test resulted in; U-statistic=246.0, p-value=0.4, and indicates no significant difference between the distributions because the critical value for the samples is 56 and the obtained U is larger than that.

Of the 12 trips with open windows presented in Table 6, two buses were using biogas and 10 of them used biodiesel.

On one occasion, a trip with closed sunroof was followed by a trip with open sunroof, both using the same fuel. This event is plotted in Figure 14 and show different profiles along the route but the resulting mean concentrations for the trips were 247 ng/m^3 for closed and 245 ng/m^3 open.

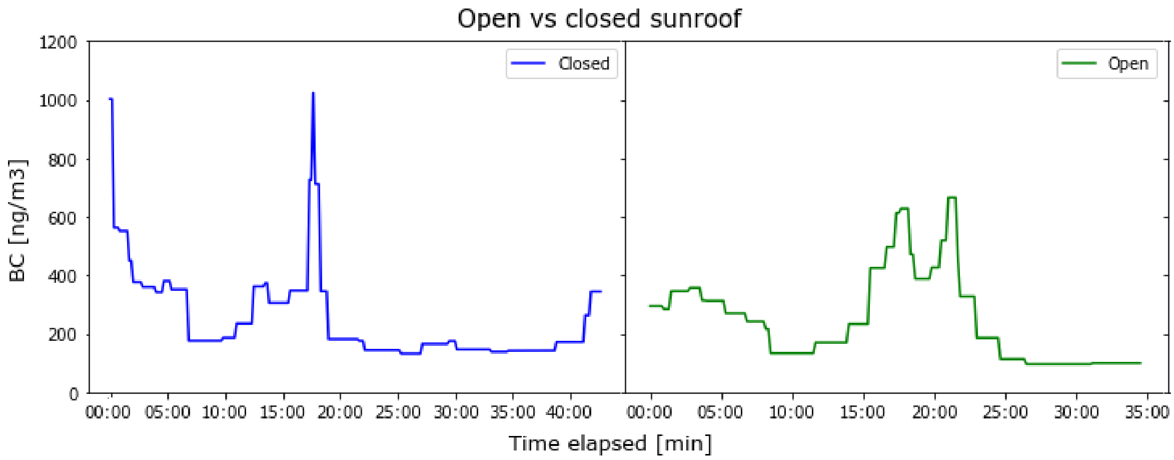

Figure 14. Timeline with concentrations for two trips with closed and open sunroof.

Discussion

Summary

The measurements in the study displayed a large variation in spatial distribution of peaks in concentrations occurring on several places. Especially in the locations defined as Hot spots where longer stops were made, these locations on average experienced a 42% increase compared to the overall total concentrations. Morning trips for biodiesel showed the most noticeable difference compared to the other time intervals with approximately twice as high mean concentrations, although strongly dependent on three specific trips. In general, the two fuels compared did not show a significant difference in mean concentrations but the maximum value for biodiesel exceed the biogas as well as had a wider distribution skewed towards higher values seen by the lower median. The comparison between trips with open and closed sunroof did not show any statistical significant difference in distributions, even though the overall mean values indicated 19% higher concentrations for trips with open sunroof.

Spatial distribution

The spatial distributions of BC-concentrations vary widely along the route with high concentrations in different parts of the trip depending on fuel and direction. The regression analysis between the different combinations of fuel and direction tells that it is very precarious to determine a significant relationship, making it hard to point out with certainty where high concentrations always occurs. Specific events, unique to one trip can have a large influence on the overall result. This is for example reflected in Figure 6d where only two trips show exaggerated values in the beginning of the trip and dominates the section of the trip. There are, however, some interesting results to point out from the spatial distribution.

The pattern that high concentrations appear in the beginning of each trip seems reoccurring independent of direction and fuel. This may be due to the selection in start and end point, the closest station to Stadion is the north eastern bus hub for Stockholm where buses covering areas outside of Stockholm have their station which are all fuelled with biodiesel. The street is also a highly trafficked street with around 26,000 vehicles passing every day (Stockholm Stad, 2020). High values are noticed in this station on many occasions, but because there were no repeatedly long stops during the campaign it did not qualify as a hot spot due to the stops being very short and not comparable with the other stations that qualified. On the other end of the route, trips starting at Skanstull also follow a pattern of increased concentrations with values above 600 ng/m^3. Skanstull is a bus stop, like Stadion, in an intensely trafficked street and this might influence the concentrations in this location as well. Intense traffic cannot be the only reason to why the bus seems highly affected in these parts of the route though, if the perspective is shifted, and both Skanstull and Stadion are viewed as end stops, the concentrations are lower much lower. This raises questions on why a street that experience high values in one direction, do not in the opposite. An explanation might be that as the bus gets closer to the end station less travellers are on-board meaning fewer stops and thus fewer openings of doors to allow polluted air from the traffic around to enter. In reverse, as the bus is on its way towards the centre of the city, it was noted that more people tend to get onboard causing more stops. No previous study mentions direction of travel as a potential factor to influence in-cabin concentrations, but studies confirm that driving with many starts and stops show increased values (Targino et al., 2018; Zuurbier et al., 2010).

Another explanation to the variation in concentrations depending on direction of travel could be the wind direction. As the bus travels two directions, the door pairs are facing opposite sides of the street and if the wind direction is the same during both trips it will have different impacts on the two separate stops. On one side, the air might be blown into the cabin from a wind adjacently directed towards the side where the door pairs open. On the way back, when the door pairs face the other way, the bus itself might act as windshield blocking the air to enter the cabin immediately. If the hold up is long enough, the wind might eventually penetrate the cabin even though the door pair is faced away from the wind, but for shorter stops the difference might be larger.

The locations of reoccurring events like long hold ups and driver shifts, marked out with (A-D) in Figure 6, seem to experience repeatedly elevated concentrations. This is implied by the increasing concentrations close to these locations and is also confirmed in the statistical summary for hot spots where all mean values exceed the overall mean. With the only one exception in Södra Station, location D, these places are in intensely trafficked streets with several bus lines covering the station, meaning that fumes from both the exhaust of buses idling at the bus stop as well as from passing surrounding traffic may enter the cabin. When comparing the trips including long stops at hot spots and trips without significantly long stops, it is necessarily not the case that only the long stops undergo large increases. There are events where long stops show no peak at all as well as there are occasions where a stop that was not noticed as a long stop see a peak, although it is more frequently occurring when the stop is longer. From the results it can be extracted that wind direction and surrounding traffic is a major factor when the bus is idling. Both Odenplan (A) and Fridhemsplan (B) have an east-west direction, peaks in both places are more frequent when the wind direction is north west, which was the most frequent wind direction overall in the period, and the driving direction is towards Skanstull. This makes the door pairs exposed adjacently to the wind direction and has previously been established by Zhang et al. (2013) as a contributing factor to in-cabin pollution. Hornstull (C) and Södra Station (D) are in north-south direction but have a denser street geometry surrounding them. This could indicate that there is a risk of poor street ventilation when winds are stopped by buildings and thus show increased values on certain occasions. The potential impact of poor street ventilation has been discussed by Targino et al. (2020). Overall, the finding that bus stations have large impact on in-cabin concentrations agrees with those of Betancourt et al. (2019) and Targino et al. (2018). An uncertainty in the plots of the spatial distribution is the variation in length of the trips averaged together. Trips with outlying lengths, larger than three-minute difference from the average, has been excluded. This means that the spatial distribution is sufficient in telling where concentrations tend to peak while it is not sufficient in telling precise concentrations at these locations. The findings that long stops might experience higher concentrations is supported by the randomly selected trip where speed is put in relation to concentrations, which show a peak during a time of no speed at all.

Daily variability

Evaluating the day-to-day differences resulted in a varied distribution with no significant patterns to follow. The most common trip to have the highest value for one day was the morning trips. The results suggest that this mainly was caused by surrounding traffic in combination with specific meteorological conditions without connection to the time of day. Wind speed was shown to generally be lower in the morning and slowly increase during the day but the occasions that presented the highest values experienced wind speeds of about 6-7 m/s compared to a mean 4.5 m/s for the same interval. A low wind speed indicates a less turbulent airflow and therefore less well-mixed air and would be expected to result in higher in-cabin concentrations with a fixed wind direction when compared to a more turbulent flow. The results presented did not support that assumption as trips with similar wind directions but with different wind speeds showed a tendency towards higher values when wind speeds were higher. Wind speeds are measured at different locations than the locations of comparison and should thus be associated with large variability as wind is affected by external factors like street geometry and nearby buildings.

Type of fuel and self-pollution

Overall, the results suggest that there are no significant differences in the mean concentrations between buses fuelled with biodiesel and biogas. No comparison has previously been done with biodiesel and biogas, but other studies that have compared diesel-buses with environmentally friendlier alternatives like biodiesel (Targino et al., 2020) and electrical (Zuurbier et al., 2010;

Betancourt et al., 2019) and found significant reductions of in-cabin concentrations. The results from the comparison between the two fuels used in this study suggests that the biodiesel buses have a larger variability in the pollutants. This is derived from the skewed distribution and the result that the maximum value obtained in a biodiesel bus exceed the maximum value for biogas with a factor of two. It is associated with large uncertainties where the variability in concentrations for biodiesel comes from and the only difference between the two fuels is the observed ability for biodiesel to obtain contamination from their own exhausts. It is however not well-determined how large part of the peaks in concentration comes from surrounding traffic and how much that comes from the bus's own exhausts.

The peaks in concentrations at bus stops could, beside surrounding traffic, be explained by self-pollution. When the bus is idling, the concentrations of BC from the exhaust is mixed with the air around the bus, and combined with a wind direction that comes from straight behind the bus, the exhausts might enter the cabin as described by Zhang et al. (2013). What the results suggest however, is that the concentrations of BC in the exhaust-air might be low and not have a larger impact than the urban background. By using the suggestion that dilution ratios of 1000 or larger are reached after only one to two seconds after the exhaust-air leave the tailpipe from Kittelson (2001), the concentrations behind the buses in this study can be estimated to approximately 30 ng/m^3 and 130 ng/m^3 for biogas and biodiesel, respectively. Results from other studies confirm that the concentrations behind buses fuelled with CNG and of class Euro VI are similar to those of urban background measurements (Järvinen et al., 2019; Pirjola et al., 2015). This would not affect the in-cabin concentrations significantly if the bus made a short stop, but the possibility of accumulating the pollutants during longer stops might be a source to self-contamination. It is perhaps more likely that the combination of several buses idling in the larger bus stops together contribute to a polluted environment that causes the peaks during the long stops, but more studies on the situations of idling at bus stops would be required to get a better understanding of the potential self-pollution during these stops.

There exist peaks in biogas-buses during stop-and-go driving as well, indicating that peaks in concentrations during trips with biodiesel necessarily do not need to origin from their own exhaust. What is found in this study does, however, suggests that during traffic situations where many start and stops are made, and wind direction comes straight from behind the exhausts from the bus can enter the cabin. This has also been shown by Behrentz et al. (2004) and Zhang et al. (2013). The calculations of how large part of concentrations that can be explained by self-pollution showed 2.5% for biogas and 10% for biodiesel, in comparison to that Behrentz et al. (2004) and Zuurbier et al. (2010) found 25% and 30% for diesel trips. This discrepancy may be due to the differences in what fuels are used, as well as the age and euro-class of the buses. Because HBEFA does not distinguish between biodiesel or diesel or when both are of class Euro VI, this leaves room for uncertainties as no studies comparing the two has been made, the closest finding on this subject is the comparison between diesel of Euro II/III and biodiesel of Euro V by Targino et al. (2020), which showed a large difference in in-cabin pollution. This is not entirely applicable to this study since the differences between the classes are too large but indicates that there could be a difference between emissions factors of diesel and biodiesel with Euro VI. Another uncertainty related to the studied buses concerns the different ages of the buses. Production year range between 2011 and 2018 for the biogas buses, overall wear after many years of duty may influence the particulate filters and concentrations in engine exhaust. The assumption that the CNG driven buses are identical along with the values in volumetric flow rate of air from the exhaust stated by Behrentz et al. (2004) implies uncertainties in precision of self-contamination from particularly biogas buses, but biodiesel as well even though the time span of production years is less stretched.

All calculations on self-pollution leave room for uncertainties, mainly because this study itself did not measure tailpipe concentrations nor have access to detailed data on each engine used. The approximations on the volumetric flow rate from the tailpipe are calculated on different bus models as well as given without assumptions on temperature and pressure. The fraction, θ, of BC from the exhaust that enters the cabin is also an estimate made in Behrentz et al. (2004) and is an average for one bus trip, which should be considered with uncertainty in this study because of variations in bus models and year of production.

Effects of open or closed window

Driving with an open window allows for higher risk of penetration of exhausts from surrounding traffic compared to driving with a closed window. This is indicated by the large variation in concentrations for trips with the sunroof open, and even though the mean concentrations do not exceed the trips with closed sunroof by more than 19%, it allows for a potential source of unwanted polluted impacts from surrounding traffic as well as self-pollution. The findings that driving with an open window generates higher in-cabin concentrations are supported by Li et al. (2015) but opposed by the study by Behrentz et al. (2004) and Li et al. (2017) who found that driving with closed windows experienced 55% higher concentrations than open. An effect of driving with open windows is the reduction in age of air investigated by Li el al., (2017) to examine ventilation rates. Their findings suggest that the age of air for a bus driving 32 km/h, on average had approximately three times older air in the rear end of the bus when all windows were closed compared when the middle windows were open. This means that in parts of the route where polluted air has entered the cabin at a bus stop and is kept inside the bus for a longer period. This could be the explanation of the in-cabin concentrations between the two bus stops Västerbroplan and Högalidsgatan where a long bridge of constant driving separates the stations. There are uncertainties regarding bus model and placement of windows between the buses used in this study and the ones by Li et al. (2017), but similar air flow patterns inside the cabin should apply, especially in the case of closed windows. The comparison between the two trips sampled directly after each other, where one trip had open sunroof and the other one had closed, does not support that driving with open windows must infer increased concentrations. The trips were in opposite direction and this might have influenced the results because of the meteorology.

Limitations

The study was conducted during the covid-19 pandemic and the number of vehicles in traffic was probably significantly reduced compared to normal traffic. The limitation in not being able to access daily traffic rates makes it difficult to evaluate potential daily differences in surrounding traffic. Also due to covid-19 and public safety reasons, sessions were kept shorter than expected and to hours where fewest possible passengers travelled with the bus to avoid overcrowding. There might have been differences from a normal period in how the bus drivers handled opening and closing of doors at bus stops, all passengers entered through the middle and rear door pairs instead of in the front. Additional limitations is the lack of accessibility to information on the ratios of the blends for the fuels utilised which may have an impact on the results, and further details on the performance of the engines regarding filters and differences between years.

Conclusions

This study tried to i) compare in-cabin concentrations of buses with differences in their BC emissions ii) identify factors that impact concentrations of black carbon inside the micro-environment of buses used in the public transport system of Stockholm, Sweden. By performing black carbon sampling on 55 bus trips, the research can conclude a large variability in both a daily and diurnal time scale. The method allowed for evaluation of various driving situations and observation of reoccurring events along the route, a route that experienced different types of driving and intensities in traffic. From the findings it can be derived that buses idling in bus stops with open doors are at greater risk of seeing elevated concentrations, largely depending on outer conditions like surrounding traffic and wind direction. The occurrence of self-contamination is not strongly evident but might be an explanation to the increase of 3.6% in total average concentrations and skewed distribution for buses fuelled with biodiesel compared to those fuelled with biogas. The findings suggest that the two fuels compared in this study does not show considerable differences and that on the occasions of large difference it was mainly due to surrounding conditions like traffic and meteorology. Idling with closed doors in bus stops could reduce the risk of allowing polluted air into the cabin, although there are events where idling with closed doors have shown elevated values as well. More studies during real traffic situations in what affects the concentrations specifically during idling would be required to get a better understanding of how to reduce the risks even further.

Acknowledgements

I want to thank supervisor Christer Johansson for the support and expertise during the study as well as access to the instruments needed to perform the study. I also want to thank Daniel Schlesinger for providing Python-code to make the GPS-visualisations possible and Paul Ziegler for providing the GPS equipment.

References

1. Behrentz, E., Fitz, D. R., Pankratz, D. V., Sabin, L. D., Colome, S. D., Fruin, S. A., & Winer, A. M., 2004. Measuring self-pollution in school buses using a tracer gas technique. ATMOSPHERIC ENVIRONMENT, 23, 3735.
2. Bond, T., Doherty, S., Fahey, D., Forster, P., Berntsen, T., DeAngelo, B., Flanner, M., Ghan, S., Kärcher, B., Koch, D., Kinne, S., Kondo, Y., Quinn, P., Sarofim, M., Schultz, M., Schulz, M., Venkataraman, C., Zhang, H., Zhang, S., Bellouin, N., Guttikunda, S., Hopke, P., Jacobson, M., Kaiser, J., Klimont, Z., Lohmann, U., Schwarz, J., Shindell, D., Storelvmo, T., Warren, S. and Zender, C., 2013. Bounding the role of black carbon in the climate system: A scientific assessment. Journal of Geophysical Research: Atmospheres, 118(11), pp.5380-5552.
3. Carvalho, A.M., Krecl, P. & Targino, A.C., 2018. Variations in individuals' exposure to black carbon particles during their daily activities: a screening study in Brazil. Environ Sci Pollut Res 25, 18412–18423. https://doi.org/10.1007/s11356-018-2045-8
4. Cohen, A., Brauer, M., Burnett, R., Anderson, H., Frostad, J., Estep, K., Balakrishnan, K., Brunekreef, B., Dandona, L., Dandona, R., Feigin, V., Freedman, G., Hubbell, B., Jobling, A., Kan, H., Knibbs, L., Liu, Y., Martin, R., Morawska, L., Pope, C., Shin, H., Straif, K., Shaddick, G., Thomas, M., van Dingenen, R., van Donkelaar, A., Vos, T., Murray, C. and Forouzanfar, M., 2017. Estimates and 25-year trends of the global burden of disease attributable to ambient air pollution: an analysis of data from the Global Burden of Diseases Study 2015. The Lancet, 389(10082), pp.1907-1918. https://doi.org/10.1016/s0140-6736(17)30505-6
5. Fruhstorfer, P. and Niessner, R., 1994. Identification and classification of airborne soot particles using an automated SEM/EDX. Mikrochimica Acta, 113(3-6), pp.239-250. https://doi.org/10.1007/bf01243614
6. Grahame, T., Klemm, R. and Schlesinger, R., 2014. Public health and components of particulate matter: The changing assessment of black carbon. Journal of the Air & Waste Management Association, 64(6), pp.620-660.
7. Hagler, G., Yelverton, T., Vedantham, R., Hansen, A. and Turner, J., 2011. Post-processing Method to Reduce Noise while Preserving High Time Resolution in Aethalometer Real-time Black Carbon Data. Aerosol and Air Quality Research, 11(5), pp.539-546. https://doi.org/10.4209/aaqr.2011.05.0055
8. Ham, W., Vijayan, A., Schulte, N. and Herner, J., 2017. Commuter exposure to PM2.5, BC, and UFP in six common transport microenvironments in Sacramento, California. Atmospheric Environment, 167, pp.335-345. https://doi.org/10.1016/j.atmosenv.2017.08.024
9. Hansen, A., Rosen, H. and Novakov, T., 1984. The aethalometer — An instrument for the real-time measurement of optical absorption by aerosol particles. Science of The Total Environment, 36, pp.191-196. https://doi.org/10.1016/0048-9697(84)90265-1
10. Hinds, W. C. (1999) Aerosol Technology: Properties, Behavior, and Measurement of Airborne Particles. New York: Wiley-Interscience. Available at: http://search.ebscohost.com.ezp.sub.su.se/login.aspx?direct=true&db=edsebk&AN=531512&site=eds-live&scope=site (Accessed: 3 May 2020).
11. Järvinen, A., Timonen, H., Karjalainen, P., Bloss, M., Simonen, P., Saarikoski, S., Kuuluvainen, H., Kalliokoski, J., Dal Maso, M., Niemi, J., Keskinen, J. and Rönkkö, T., 2019. Particle emissions of Euro VI, EEV and retrofitted EEV city buses in real traffic. Environmental Pollution, 250, pp.708-716.
12. Kittelson, D., 2001. RECENT MEASUREMENTS OF NANOPARTICLE EMISSIONS FROM ENGINES.
13. Li, B., Lei, X., Xiu, G., Gao, C., Gao, S. and Qian, N., 2015. Personal exposure to black carbon during commuting in peak and off-peak hours in Shanghai. Science of The Total Environment, 524-525, pp.237-245.
14. Li, F., Lee, E. S., Zhou, B., Liu, J., & Zhu, Y., 2017. Effects of the window openings on the micro-environmental condition in a school bus, Atmospheric Environment, 167, pp. 434–443. doi: 10.1016/j.atmosenv.2017.08.053.
15. Merritt, A., Georgellis, A., Andersson, N., Bero Bedada, G., Bellander, T. and Johansson, C., 2019. Personal exposure to black carbon in Stockholm, using different intra-urban transport modes. Environmental Epidemiology, 3, pp.269-270. https://doi.org/10.1097/01.ee9.0000608876.42369.6d
16. Morales Betancourt, R., Galvis, B., Rincón-Riveros, J., Rincón-Caro, M., Rodriguez-Valencia, A. and Sarmiento, O., 2019. Personal exposure to air pollutants in a Bus Rapid Transit System: Impact of fleet age

and emission standard. Atmospheric Environment, 202, pp.117-127. https://doi.org/10.1016/j.atmosenv.2019.01.026

17. Naturvårdsverket. 2020. Luftföroreningar Och Dess Effekter. [online] Available at: <https://www.naturvardsverket.se/Sa-mar-miljon/Klimat-och-luft/Luftfororeningar/> [Accessed 3 May 2020].
18. Nogueira, T., Dominutti, P., Vieira-Filho, M., Fornaro, A. and Andrade, M., 2019. Evaluating Atmospheric Pollutants from Urban Buses under Real-World Conditions: Implications of the Main Public Transport Mode in São Paulo, Brazil. Atmosphere, 10(3), p.108. https://doi.org/10.3390/atmos10030108
19. Pirjola, L., Dittrich, A., Niemi, J., Saarikoski, S., Timonen, H., Kuuluvainen, H., Järvinen, A., Kousa, A., Rönkkö, T. and Hillamo, R., 2015. Physical and Chemical Characterization of Real-World Particle Number and Mass Emissions from City Buses in Finland. Environmental Science & Technology, 50(1), pp.294-304.
20. Seinfeld, J. and Pandis, S., 2016. Atmospheric Chemistry And Physics: From Air Pollution To Climate Change, 3R. John Wiley & Sons.
21. SL (2018). SL och länet 2018. SL.
22. Stockholm Stad. 2020. Trafikflöden i Stockholm. [online] Available at: <http://miljobarometern.stockholm.se/trafik/motorfordon/trafikfloden-i-stockholm/> [Accessed 15 May 2020]
23. Targino, A.C., Rodrigues, M.V.C., Krecl, P. et al., 2018 Commuter exposure to black carbon particles on diesel buses, on bicycles and on foot: a case study in a Brazilian city. Environ Sci Pollut Res 25, 1132–1146. https://doi.org/10.1007/s11356-017-0517-x
24. Targino, A., Krecl, P., Cipoli, Y., Oukawa, G. and Monroy, D., 2020. Bus commuter exposure and the impact of switching from diesel to biodiesel for routes of complex urban geometry. Environmental Pollution, 263, p.114601. https://doi.org/10.1016/j.envpol.2020.114601
25. World Health Organization. (2016). Ambient air pollution: a global assessment of exposure and burden of disease. World Health Organization.
26. Zhang, Q., Fischer, H. J., Weiss, R. E., & Zhu, Y., 2013. Ultrafine particle concentrations in and around idling school buses. Atmospheric Environment, 69, 65–75. https://doi-org.ezp.sub.su.se/10.1016/j.atmosenv.2012.12.015
27. Zuurbier, M., Hoek, G., Oldenwening, M., Lenters, V., Meliefste, K., van den Hazel, P. and Brunekreef, B., 2010. Commuters' Exposure to Particulate Matter Air Pollution Is Affected by Mode of Transport, Fuel Type, and Route. Environmental Health Perspectives, 118(6), pp.783-789. https://doi.org/10.1289/ehp.0901622

Appendix A

2/4						
Statistics	Biogas A	Biogas B	Biodiesel A	Biodiesel B	Street Level	Background
P5	134	127	121	126	312	76
P25	156	162	172	183	322	83
Median	197	214	191	216	335	96
P75	290	284	282	381	388	98
P95	506	415	405	527	425	117
Mean	244	232	230	268	358	95
SD	118	88.3	90.0	125.9	46.8	16.0
Maximum	535	488	481	546	435	122

7/4						
Statistics	Biogas A	Biogas B	Biodiesel A	Biodiesel B	Street Level	Background
P5	563	194	932	443	1089	960
P25	612	203	1022	500	1157	1066
Median	677	239	1189	608	1577	1315
P75	734	374	1921	863	1602	1339
P95	839	589	2207	1045	1994	1466
Mean	684	306	1445	686	1500	1230
SD	91	127	483	210.8	365.4	202.9
Maximum	983	610	2624	1132	2092	1498

8/4						
Statistics	Biogas A	Biogas B	Biodiesel A	Biodiesel B	Street Level	Background
P5	154	163	205	143	429	154
P25	228	228	326	150	445	166
Median	283	283	414	206	500	194
P75	412	325	465	271	524	259
P95	571	509	654	395	558	295
Mean	324	295	404	225	492	215
SD	130.7	114.8	123.7	89.3	51.4	58.1
Maximum	638	930	734	554	566	304

9/4						
Statistics	Biogas A	Biogas B	Biodiesel A	Biodiesel B	Street Level	Background
P5	43	92	113	58	283	69
P25	48	123	130	59	325	70

Median	119	204	174	183	410	85
P75	157	302	302	266	478	86
P95	346	504	786	502	489	102
Mean	128	230	281	195	395	83
SD	97.1	119.8	247.7	137.3	85.3	13.3
Maximum	351	534	1373	538	492	106
			14/4			
Statistics	Biogas A	Biogas B	Biodiesel A	Biodiesel B	Street Level	Background
P5	96	144	250	85	247	91
P25	222	191	454	176	282	100
Median	274	284	682	305	283	100
P75	376	395	1051	357	355	107
P95	757	1495	1764	877	414	118
Mean	325	451	806	332	317	103
SD	200.4	687.7	488.1	350.4	66.9	10.6
Maximum	975	4580	2407	2808	428	121
			15/4			
Statistics	Biogas A	Biogas B	Biodiesel A	Biodiesel B	Street Level	Background
P5	89	117	561	68	270	103
P25	155	162	1178	81	305	123
Median	294	339	1476	109	308	123
P75	342	560	1816	282	353	143
P95	396	1025	2241	490	398	148
Mean	261	412	1466	193	327	127
SD	108.2	287.4	508.3	145.8	50.4	18.3
Maximum	468	1185	2757	571	410	150
			16/4			
Statistics	Biogas A	Biogas B	Biodiesel A	Biodiesel B	Street Level	Background
P5	320	-	21	74	300	0
P25	368	110	21	91	318	0
Median	589	250	132	143	351	84
P75	900	451	172	195	412	99
P95	1364	1022	513	234	474	113
Mean	691	310	154	152	373	60
SD	363.6	316.8	160.0	95.6	70.2	50.2
Maximum	1988	1177	780	967	490	117
			20/4			
Statistics	Biogas A	Biogas B	Biodiesel A	Biodiesel B	Street Level	Background

P5	180	161	143	189	515	159
P25	302	248	183	229	528	194
Median	531	269	236	281	646	217
P75	624	319	296	328	774	228
P95	995	1053	366	420	932	391
Mean	539	407	241	288	686	244
SD	306.1	464.3	75.4	82.8	171.0	97.4
Maximum	2202	3604	452	524	971	432

21/4

Statistics	Biogas A	Biogas B	Biodiesel A	Biodiesel B	Street Level	Background
P5	129	121	44	100	517	108
P25	206	134	44	135	728	123
Median	255	178	81	192	828	144
P75	438	214	185	287	1135	163
P95	489	552	352	490	1510	211
Mean	297	220	127	253	952	151
SD	140.4	172.6	106.3	201.6	390.4	40.8
Maximum	682	1017	535	1308	1603	223

22/4

Statistics	Biogas A	Biogas B	Biodiesel A	Biodiesel B	Street Level	Background
P5	-	163	205	143	429	154
P25	-	228	326	150	445	166
Median	-	283	414	206	500	194
P75	-	325	465	271	524	259
P95	-	509	654	395	558	295
Mean	-	295	404	225	492	215
SD	-	114.8	123.7	89.3	51.4	58.1
Maximum	-	930	734	554	566	304

27/4

Statistics	Biogas A	Biogas B	Biodiesel A	Biodiesel B	Street Level	Background
P5	119	74	102	124	187	95
P25	150	145	120	167	210	101
Median	197	217	156	241	264	129
P75	273	408	210	347	283	137
P95	468	614	376	808	347	188
Mean	231	274	213	284	260	132
SD	129.0	171.4	191.4	178.7	63.2	38.0
Maximum	922	827	1442	887	363	201

28/4						
Statistics	Biogas A	Biogas B	Biodiesel A	Biodiesel B	Street Level	Background
P5	53	86	70	81	494	103
P25	53	110	109	105	508	125
Median	211	115	261	132	539	130
P75	408	310	393	350	544	137
P95	558	359	530	932	639	137
Mean	237	189	253	268	549	125
SD	183.8	122.2	162.1	255.9	60.4	14.8
Maximum	659	629	689	1104	663	137
29/4						
Statistics	Biogas A	Biogas B	Biodiesel A	Biodiesel B	Street Level	Background
P5	127	483	92	60	514	175
P25	147	679	118	134	652	191
Median	259	834	166	255	653	200
P75	467	1086	301	368	711	223
P95	809	1384	482	674	724	258
Mean	330	876	216	288	644	210
SD	217.5	280.1	121.6	194.0	87.9	33.0
Maximum	1052	1518	507	1020	727	267
30/4						
Statistics	Biogas A	Biogas B	Biodiesel A	Biodiesel B	Street Level	Background
P5	133	252	142	88	384	151
P25	239	347	178	198	568	179
Median	290	521	237	290	601	191
P75	379	852	417	378	775	232
P95	452	2905	565	595	1185	252
Mean	298	806	301	396	714	201
SD	94.6	832.1	159.4	836.7	318.6	39.8
Maximum	516	4330	745	8739	1287	258

Table 7. Statistical summary over the daily variation. The notation "A" represents the starting point Stadion, and "B" represents trips with starting point Skanstull.

Appendix B

Meteorological Data						
Date	Time of day	Relative Humidity [%RH]	Temperatur [°C]	Precipitation [mm/hour]	Wind Speed [m/s]	Wind direction [°]
	09:00	65.1525	5.11525	0	7.27	245
	10:00	57.635	5.94801	0	6.77	246.6
2/4	11:00	47.38	7.3975	0	6.018	227.7
	12:00	45.3125	8.1875	0	6.89	217.3
	13:00	43.945	8.77499	0	8.31	223.4
	09:00	61.145	8.38249	0	3.019	199.4
	10:00	52.7075	10.67	0	3.962	225.1
7/4	11:00	62.78	9.745	0.19	3.565	229.3
	12:00	74.9	9.07001	0	7.55	257.7
	13:00	67.5675	10.6425	0	8.45	254.6
	09:00	57.9575	7.91	0	3.786	221.9
	10:00	53.7775	9.3	0	3.964	229.9
8/4	11:00	49.3825	10.45	0	5.962	228
	12:00	45.81	11.605	0	4.689	226.5
	13:00	40.8525	12.6475	0	6.425	231.3
	09:00	42.835	7.74	0	4.47	322.4
	10:00	36.6025	7.8325	0	4.382	323.5
9/7	11:00	32.3	8.99501	0	4.447	300.9
	12:00	28.78	9.5	0	4.637	306.9
	13:00	26.6025	9.4825	0	5.658	309.2
	09:00	47.4775	2.4185	0	6.036	304.7
	10:00	41.5775	4.07	0	6.767	313.6
14/4	11:00	36.765	5.31775	0	7.21	315.2
	12:00	34.2025	5.42525	0	6.065	305.6
	13:00	31.12	6.2645	0	7.29	296.1
	09:00	69.7676	6.76675	0	6.114	279.5
	10:00	59.735	8.545	0	5.546	294.4
15/4	11:00	47.37	10.075	0	6.88	304.5
	12:00	39.8725	10.98	0	5.163	304

	13:00	34.135	11.8	0	6.129	291.1
	09:00	39.54	7.655	0	8.74001	299.7
	10:00	37.635	8.065	0	8.74001	313.9
16/4	11:00	35.235	8.54251	0	8.58	321.7
	12:00	33.9975	8.7675	0	6.394	315.6
	13:00	29.09	9.72749	0	7.7	318.9
	09:00	61.8575	8.3725	0	2.079	328.7
	10:00	55.9675	10.1025	0	2.127	278.1
20/4	11:00	51.9475	11.185	0	2.85	292.5
	13:00	42.8525	13.63	0	2.34	323.9
	12:00	46.4725	12.8225	0	2.558	289.7
	09:00	50.665	9.7075	0	2.43	357.5
	10:00	43.2625	11.535	0	2.028	327.5
21/4	11:00	39.3975	12.9125	0	3.515	350.7
	13:00	38.2625	14.4825	0	3.168	19.56
	12:00	38.215	13.85	0	3.521	31.95
	09:00	50.3625	10.3875	0	3.978	1.587
	10:00	49.085	11.1375	0	4.141	13.78
22/4	11:00	45.33	12.4225	0	2.189	1.694
	13:00	36.415	14.2325	0	3.771	9.64999
	12:00	41.9925	13.5625	0	4.366	28.29
	09:00	36.745	7.87251	0	3.913	85.2
	10:00	34.4775	7.8425	0	4.356	118.2
27/4	11:00	34.3975	8.19751	0	4.156	88.3
	12:00	34.535	8.25999	0	4.197	113
	13:00	31.9775	8.88	0	4.465	88.8
	09:00	95.525	1.85075	0	4.349	35.2
	10:00	94.975	2.061	0.38	4.902	35.38
28/4	11:00	94.9	1.82175	0.76	5.385	36.64
	13:00	90.2001	2.775	0	4.292	42.09
	12:00	91.3	2.43575	0.19	4.359	35.16
	09:00	67.7125	2.83525	0	4.365	340.1
	10:00	67.0026	2.97425	0	3.584	331.4
29/4	11:00	60.15	3.85575	0	4.613	23.14
	12:00	58.16	4.16375	0	4.012	347.7
	13:00	52.45	4.76075	0	5.336	24.38
	09:00	85.475	2.72475	0	2.937	66.62

	10:00	72.97	4.1815	0	2.766	58.19
30/4	11:00	65.9175	5.26525	0	2.605	39.51
	13:00	54.3425	6.3175	0	4.886	102.4
	12:00	54.5775	6.189	0	4.923	88.1

Table 8. Summary of the meteorological data from the sampling days.

Stockholm University
SE-106 91 Stockholm
Telefon/Phone: 08 – 16 20 00
www.su.se

Stockholms
universitet